Acta Pharmacologica Sinica

www.nature.com/aps

ARTICLE

Sodium propionate exerts anticancer effect in mice bearing breast cancer cell xenograft by regulating JAK2/STAT3/ROS/p38 MAPK signaling

Hyun-Soo Park[1], Joo-Hui Han[1], Jeong Won Park[2], Do-Hyung Lee[1], Keun-Woo Jang[1], Miji Lee[1], Kyung-Sun Heo[1] and Chang-Seon Myung[1]

Propionate is a short-chain fatty acid (SCFA) mainly produced from carbohydrates by gut microbiota. Sodium propionate (SP) has shown to suppress the invasion in G protein-coupled receptor 41 (GPR41) and GPR43-overexpressing breast cancer cells. In this study we investigated the effects of SP on the proliferation, apoptosis, autophagy, and antioxidant production of breast cancer cells. We showed that SP (5−20 mM) dose-dependently inhibited proliferation and induced apoptosis in breast cancer cell lines JIMT-1 (ER-negative and HER2-expressing) and MCF7 (ER-positive type), and this effect was not affected by PTX, thus not mediated by the GPR41 or GPR43 SCFA receptors. Meanwhile, we demonstrated that SP treatment increased autophagic and antioxidant activity in JIMT-1 and MCF7 breast cancer cells, which might be a compensatory mechanism to overcome SP-induced apoptosis, but were not sufficient to overcome SP-mediated suppression of proliferation and induction of apoptosis. We revealed that the anticancer effect of SP was mediated by inhibiting JAK2/STAT3 signaling which led to cell-cycle arrest at G_0/G_1 phase, and increasing levels of ROS and phosphorylation of p38 MAPK which induced apoptosis. In nude mice bearing JIMT-1 and MCF7 cells xenograft, administration of SP (20 mg/mL in drinking water) significantly suppressed tumor growth by regulating STAT3 and p38 in tumor tissues. These results suggest that SP suppresses proliferation and induces apoptosis in breast cancer cells by inhibiting STAT3, increasing the ROS level and activating p38. Therefore, SP is a candidate therapeutic agent for breast cancer.

Keywords: sodium propionate; breast cancer; JAK2; STAT3; ROS; p38 MAPK

Acta Pharmacologica Sinica (2021) 42:1311–1323; https://doi.org/10.1038/s41401-020-00522-2

INTRODUCTION

Breast cancer is the second-leading cause of cancer-related death in women and exhibits abnormal proliferation, invasion, and evasion of apoptosis [1, 2]. When cell cycle regulation is dysfunctional and apoptosis is inhibited, cancers can be aggravated [3, 4]. Breast cancer can be subclassified based on gene expression, such as the presence or absence of the estrogen receptor (ER), human epidermal growth factor receptor 2 (HER2) expression and triple-negative status (ER-, progesterone receptor-, HER2-) [2, 5]. Thus, investigating the responses of different subtypes is important for understanding the therapeutic efficacies of pharmacologic tools.

Although reactive oxygen species (ROS) production in cancer cells is greater than in healthy cells due to metabolic and hypoxia stresses, cancer cells also produce ROS scavengers and antioxidant enzymes (superoxide dismutase, glutathione, glutathione peroxidase, and peroxiredoxin) to maintain an appropriate level of ROS, which ameliorates oxidative stress and inhibits apoptosis, thus promoting cancer progression [6]. Autophagy is induced by various cellular stresses, such as a lack of nutrients and oxidative stress, and involves the degradation of organelles and unnecessary proteins [7, 8]. The formation of autophagosomes is initiated by the activation of the unc-51-like autophagy activating kinase 1 complex by a class III phosphoinositide 3-kinase complex containing beclin-1, and the autophagy-related protein 5 (Atg5)–Atg12 complex catalyzes microtubule-associated protein light chain 3 (LC3)-I to LC3-II maturation [9]. The increased autophagic activity in cancer cells plays an important role in tumor survival and growth [10]. Autophagy also decreases the anticancer drug-induced increase in ROS levels, causing drug resistance in cancer cells [11]. Therefore, modulation of the proliferation, apoptosis, antioxidant activity, and autophagy of cancer cells could be a therapeutic strategy for cancer.

The Janus kinase 2 (JAK2)-signal transducer and activator of transcription 3 (STAT3) signaling pathway promotes tumor growth by regulating the expression of cell cycle regulatory and antiapoptotic genes [12]. However, small-molecule inhibitors of STAT3 have not been approved by the United States Food and Drug Administration (FDA) [13]. The rapid increase and maintenance of p38 mitogen-activated protein kinase (MAPK) activity induces apoptosis in cancer cells, and p38 MAPK-deficient cells are resistant to apoptosis [14]. ROS-mediated p38 activity also induces

[1]Department of Pharmacology, Chungnam National University College of Pharmacy, Daejeon 34134, Republic of Korea and [2]Department of Lifetech.Institute, iNtRON Biotechnology, Seongnam-si 13202, Republic of Korea
Correspondence: Chang-Seon Myung (cm8r@cnu.ac.kr)
These authors contributed equally: Hyun-Soo Park, Joo-Hui Han

Received: 11 February 2020 Accepted: 24 August 2020
Published online: 24 September 2020

apoptosis in breast cancer cells [15]. However, p38 protects human melanoma cells by inhibiting ultraviolet-induced apoptosis [16]. Recent studies have focused on treating cancer by targeting combinations of proteins. BP-1-102, a novel inhibitor of STAT3, induced apoptosis and suppression of migration and invasion by inhibiting STAT3 and activation of p38 in gastric cancer [17]. Isoliquiritigenin induced apoptosis and cell cycle arrest by regulating the ROS-mediated MAPK/STAT3/nuclear factor kappa-light-chain-enhancer of activated B cells (NF-κB) pathways in hepatocellular carcinoma cells [18]. Tannic acid upregulated p38/STAT1 signaling and inhibited epidermal growth factor receptor/STAT1/3 signaling, which induces apoptosis and G_1 phase arrest in breast cancer cells [19]. However, there is insufficient evidence to support multiple modulations of STAT3 and p38 to achieve antiproliferative effects and induction of apoptosis in breast cancer cells as a treatment strategy. In addition, experimental evidence regarding the functional regulation of cancer cells is lacking.

Short-chain fatty acids (SCFAs; principally acetate, propionate, and butyrate) have fewer than six carbons and are produced from carbohydrates by gut microbiota [20]. Depending on the diet, the total concentration of SCFAs in the distal colon is 20–70 mM [21]. Among SCFAs, propionate is produced from succinate through the succinate pathway or from lactate via the acrylate pathway [22]. Propionate is an agonist of G protein-coupled receptor 41 (GPR41) and GPR43 and influenced insulin-induced glucose uptake by activating GPR41 in 3T3-L1 adipocytes and C2C12 myotubes [23]. In addition, propionate inhibited the proliferation of liver cancer cells by activating GPR43 [24] and inhibited proliferation and induced apoptosis through the GPR43-mediated signaling pathway in colon cancer cells [25]. Propionate also suppressed invasion by activating large tumor suppressor kinase 1 and inhibiting extracellular signal-regulated kinase 1/2 in GPR41- and 43-overexpressing breast cancer cells [26]. However, studies on propionate for the proliferation and apoptosis of breast cancer are lacking. Thus, we investigated the anticancer effect of sodium propionate (SP) on the proliferation, apoptosis, autophagy, and antioxidant production of breast cancer cells.

MATERIALS AND METHODS

Materials

SP, pertussis toxin (PTX), S3I-201, SB203580, *N*-acetyl-*L*-cysteine (NAC), zinc protoporphyrin IX (ZnPP), and 2′,7′-dichlorofluorescin diacetate (H_2DCFDA) were purchased from Sigma-Aldrich (Saint Louis, MO, USA). Rapamycin, 3-(4,5-dimethylthiazol-2-yl)-2,5-diphenyltetrazolium bromide (MTT), and 3-methyladenine (3-MA) were purchased from Merck Millipore (Billerica, MA, USA). [^{3}H]-thymidine was obtained from AgenBio, Ltd. (Seoul, South Korea). Anti-β-actin, anti-cyclin E1, anti-cyclin D1, anti-CDK2, anti-CDK4, and anti-proliferating cell nuclear antigen (PCNA) antibodies were purchased from AbFrontier (Geumcheon, Seoul, South Korea). Anti-phospho-retinoblastoma protein (Rb) (Ser$^{807/811}$), anti-LC3 A/B, anti-Atg12, anti-beclin-1, anti-phospho-p38, anti-p38, anti-phospho-JAK2 (Tyr$^{1007/1008}$), anti-JAK2, anti-phospho-STAT3 (Tyr^{705}), anti-STAT3, anti-poly (ADP-ribose) polymerase (PARP), anti-B-cell lymphoma 2 (Bcl-2), and anti-nuclear factor erythroid 2-related factor 2 (Nrf2) antibodies were purchased from Cell Signaling Technology, Inc. (Beverly, MA, USA). Anti-heme oxygenase 1 (HO-1) was purchased from Abcam (Cambridge, UK).

Cell culture

JIMT-1 (ER-negative and HER2-expressing), MCF7, and T47D (ER-positive type) and MDA-MB-231 (triple-negative) breast cancer cells were cultured in Dulbecco's modified Eagle's medium containing 10% (v/v) fetal bovine serum (FBS), 4.5 g/L *D*-glucose, SP, 2 mM *L*-glutamine, 100 IU/mL penicillin, and 100 μg/mL streptomycin at 37 °C in a humidified atmosphere containing 5% CO_2.

Cell proliferation and viability assays

For evaluation of the effect of SP on proliferation, cells were cultured in medium containing 10% FBS for 24 h. The cells were then seeded in 12-well plates at a density of 5×10^4 per well with or without SP (day 0). The cells were further cultured in medium with or without SP, and the cell numbers were counted every 24 h for 3 days using a hematocytometer. For determination of the effect of SP on proliferation and analysis of the underlying signaling pathways, cells were seeded in 96-well plates at a density of 3×10^3 cells per well and treated with or without SP, PTX, NAC, 3-MA, rapamycin, S3I-201, SB203580, or ZnPP for 48 h. Next, the medium was removed, and 200 μL of 5 mg/mL MTT was added for 4 h. After the MTT solution was replaced with 200 μL of dimethyl sulfoxide, the absorbance at 565 nm was measured using a microplate reader (Infinite M200 Pro; Tecan Group, Ltd., Männedorf, Switzerland).

Analysis of cell cycle progression

Cell cycle progression was analyzed using the Muse® Cell Cycle Kit (Merck Millipore, Billerica, MA, USA) according to the manufacturer's protocol. Briefly, cells were seeded in 6-well plates at a density of 1.5×10^5 cells per well and treated with or without 20 mM SP for 48 h. The cells were washed in phosphate-buffered saline (PBS) and fixed in 70% ethanol for 24 h at 4 °C. Next, the cells were mixed with kit solution (catalog no. MCH100106) and stained for 30 min at room temperature (RT) in the dark. Cell cycle progression was analyzed using a Muse™ Cell Analyzer (Merck Millipore).

Apoptosis assay

Cell apoptosis and viability were measured using the Muse® Count & Viability Assay Kit and Muse™ Annexin V & Dead Cell Kit (Merck Millipore) according to the manufacturer's protocol. In brief, cells were seeded in six-well plates at a density of 1.5×10^5 cells per well and treated with or without 20 mM SP, NAC, 3-MA, rapamycin, S3I-201, SB203580, or ZnPP for 48 h. The cells were washed in PBS, mixed with kit solution (catalog no. MCH100102 for dead cell counting; catalog no. MCH100105 for apoptosis analysis), and stained for 20 min at RT in the dark. Cell apoptosis and viability were measured using a Muse™ Cell Analyzer (Merck Millipore).

DNA synthesis assay

The [^{3}H]-thymidine incorporation assay was used to measure DNA synthesis, as described previously [26]. Cells were seeded in 24-well plates at a density of 2.5×10^4 cells per well, with or without SP. After 2 days, 2 μCi/mL [^{3}H]-thymidine was added to the medium, and the cells were incubated for 4 h. [^{3}H]-thymidine incorporation was stopped by washing with cold PBS containing 10% (v/v) trichloroacetic acid and ethanol/ether (1:1, v/v). The cells were dissolved in cold 0.5 N NaOH for 1 h; acid-insoluble [^{3}H]-thymidine was collected, mixed with 3 mL of scintillation cocktail (Ultimagold; Packard Bioscience, Meriden, CT, USA), and quantified using a liquid scintillation counter (LS3801; Beckman, Palo Alto, CA, USA).

Immunofluorescence staining

Immunofluorescence staining was performed as described previously [27]. Cells were seeded on cover slips, incubated for 24 h, and treated with or without 20 mM SP for 48 h. Next, the cells were washed in cold PBS, fixed with cold 4% formaldehyde for 20 min, and permeabilized in chilled 0.1% Triton X-100 for 2 min. After treatment with 3% bovine serum albumin (BSA) in PBS for 1 h at RT, the cells were incubated with a primary anti-phospho-Rb (Ser$^{807/811}$), anti-phospho-p38, or anti-phospho-STAT3 (Tyr^{705}) antibody overnight at 4 °C, followed by incubation with a fluorescein isothiocyanate-labeled secondary antibody for 2 h at RT. Nuclei were stained with 4′,6-diamidino-2-phenylindole, and immunofluorescence images were obtained using a super-resolution confocal laser scanning microscope (LSM 880 with Airyscan; Zeiss, Oberkochen, Germany).

Analysis of ROS generation

The intracellular ROS level was determined as described previously using H_2DCFDA [27]. After pretreatment with or without SP, NAC, S3I-201, or SB203580 for 48 h, the cells were incubated with 20 μM H_2DCFDA for 30 min at 37 °C. The intracellular ROS level was determined by measuring the fluorescence intensity using a microplate reader (Infinite F200 Pro; Tecan Group, Ltd.).

Western blot analysis

Western blotting was performed as described previously [27]. Briefly, total cell lysates were prepared using radioimmunoprecipitation assay lysis buffer (150 mM sodium chloride, 1% Triton X-100, 1% sodium deoxycholate, 0.1% sodium dodecyl sulfate [SDS], 50 mM Tris-HCl [pH 7.5], and 2 mM ethylenediaminetetraacetic acid) containing proteinase inhibitors. After incubation for 1 h at 4 °C, the cell lysates were centrifuged at 15,000 rpm for 10 min at 4 °C, and the supernatants were collected. The protein concentrations were determined using a Bicinchoninic Acid Protein Assay Kit (Pierce, Rockford, IL, USA). The proteins were subjected to SDS-polyacrylamide gel electrophoresis and transferred to a polyvinylidene fluoride membrane (Atto Corporation, Tokyo, Japan). After blocking, the membranes were incubated with primary antibodies against PCNA (1:1,000), cyclin E1 (1:1000), cyclin D1 (1:1000), CDK2 (1:1000), CDK4 (1:1000), phospho-Rb ($Ser^{807/811}$) (1:1000), PARP (1:1000), Bcl-2 (1:1000), GPR41 (1:500), GPR43 (1:1000), Nrf2 (1:1000), HO-1 (1:1000), phospho-p38, (1:1000), total-p38 (1:1000), phospho-JAK2 ($Tyr^{1007/1008}$) (1:1000), total-JAK2 (1:1000), phospho-STAT3 (Tyr^{705}) (1:1000), total-STAT3 (1:1000), and β-actin (1:2000). The membrane was washed and incubated with the corresponding horseradish peroxidase-conjugated secondary antibody, and the signals were detected using an enhanced chemiluminescence immunoblotting detection system. The protein levels were normalized to that of β-actin or the total protein level. Band intensities were quantified using Quantity One software (Bio-Rad, Hercules, CA, USA).

Xenograft tumorigenicity assay

The protocols for the use and care of experimental animals were approved by the Animal Care and Use Committee of Chungnam National University (approval number, CNU-00897). Six-week-old female athymic NCr-*nu/nu* mice were obtained from Samtako (Osan, Gyeonggi-do, South Korea). Administration of 20 mg/mL SP in drinking water was started simultaneously with injection of cells. For development of tumors from MCF7 cells, 10 μg/mL water-soluble β-estradiol (Sigma-Aldrich, Saint Louis, MO, USA) was administered in drinking water beginning 1 week before the injection of cells [28]. JIMT-1 and MCF7 (5×10^6 cells) cell suspensions (200 μL) mixed with Matrigel basement membrane matrix (BD Life Sciences, Franklin Lakes, NJ, USA) were inoculated subcutaneously into the right flank of the mice. The tumor size was measured using calipers weekly until the end of the study. The mice were euthanized, and the tumors were dissected. The tumor volume was calculated as $L \times W \times H \times 0.5236$.

Statistical analysis

Data are expressed as the mean ± standard error of the mean. Significant differences among groups were identified by one-way analysis of variance and Dunnett's test using Prism 5.01 (GraphPad Software, San Diego, CA, USA). A value of $P < 0.05$ was taken to indicate statistical significance.

RESULTS

SP inhibits the proliferation of breast cancer cells by inducing cell cycle arrest

The effect of SP on the proliferation of various breast cancer cells [JIMT-1 (ER-negative & HER2-expressing), MCF7 & T47D (ER-positive), and MDA-MB-231 (triple-negative)] was examined by cell counting assays. Cell growth was significantly reduced by 5 and 10 mM SP in a time-dependent manner regardless of cell type (Fig. 1a, e and Supplementary Fig. S1). Since SP-induced inhibition of cell proliferation in JIMT-1 and MCF-7 cells was greater than that in other cell types, hereafter, these two cells were used in further studies to measure cell viability and DNA synthesis using MTT and [^{3}H]-thymidine incorporation assays. As expected, the viability of both cell lines was significantly decreased by 0.5–20 mM SP at 48 h in a dose-dependent manner (Fig. 1b, f). Correspondingly, [^{3}H]-thymidine incorporation was decreased in the JIMT-1 and MCF7 cells in a dose-dependent manner (Fig. 1c, g). To assess cell cycle arrest in the JIMT-1 and MCF7 cells, we assayed the levels of cell cycle regulatory proteins by Western blotting, immunofluorescence, and flow cytometry using a Muse® Cell Cycle Kit. The expression levels of PCNA, cyclin E1/D1, and CDK2/4 in both cell lines were decreased by SP in a dose-dependent manner, as was the phosphorylation of Rb (Fig. 1d, h). These results were confirmed by immunofluorescence analysis of phospho-Rb (Fig. 1i, j). The population of G_0/G_1 phase cells was significantly increased and that of S and G_2/M phase cells was decreased by 20 mM SP in both cell lines (Fig. 1k, l). These results indicate that SP inhibits the proliferation of breast cancer cells by inhibiting the expression or activity of cell-cycle checkpoint proteins and suppressing DNA synthesis, resulting in arrest at G_0/G_1 phase.

SP induces cell death by inducing apoptosis in breast cancer cells

To confirm the effect of SP on apoptosis, we determined the changes in the levels of apoptotic markers and in nuclear morphology by Western blotting and immunofluorescence assays. SP resulted in an increased cleaved PARP level and decreased Bcl-2 level in both cell lines (Fig. 2a–d) in a dose-dependent manner. In addition, nuclear fragmentation was induced by 20 mM SP in the JIMT-1 and MCF7 cells (Fig. 2e, f). Next, viability and apoptosis were analyzed using the Muse® Count & Viability Kit and Annexin V & Dead Cell Kit. The proportion of dead 20 mM SP-treated JIMT-1 and MCF7 cells was significantly increased compared with that of the control cells (Fig. 2g). Moreover, the proportion of apoptotic and dead cells was significantly increased by 20 mM SP (Fig. 2h). Although SP increased the expression of GPR41, but not GPR43 (Supplementary Fig. S2a, b), the effect of SP was not affected by PTX, a $G\alpha_i$-mediated signaling inhibitor (Supplementary Fig. S2c–h). Thus, SP induces apoptosis and causes death of breast cancer cells independent of GPR41 or GPR43.

Effect of SP on autophagy in breast cancer cells

Autophagy plays an important role in the maintenance of intracellular homeostasis and viability and affects cell proliferation, migration, and differentiation [29, 30]. Cancer cells form tumors by increasing autophagy, which also confers resistance to chemotherapy [11]. To confirm the effect of SP on autophagy in breast cancer cells, we measured the levels of the autophagic markers LC3-II, beclin-1, and free Atg12 by Western blotting. SP increased the levels of LC3-II and beclin-1 and decreased that of free Atg12 at 48 h in a dose-dependent manner (Fig. 3a, b). Therefore, SP increases autophagic activity in JIMT-1 and MCF7 breast cancer cells.

To determine the role of autophagy in the SP-mediated apoptosis and inhibition of proliferation, we used 5 mM 3-MA (autophagy inhibitor) and 200 nM rapamycin (autophagy activator). The SP-induced increase in the cleaved PARP level was greater in the 3-MA-treated cells than in the control cells (SP treatment) (Fig. 3c, d). In contrast, the level of cleaved PARP was lower than that in the control group following rapamycin treatment. The regulation of autophagy by 3-MA or rapamycin might not alter the SP-mediated inhibition of proliferation. However, MTT assays showed that 3-MA significantly enhanced the SP-mediated inhibition of proliferation in both cell lines (Fig. 3e, f). In contrast, the antiproliferative activity of 20 mM SP was weakened by rapamycin in both cell lines. Similarly, the

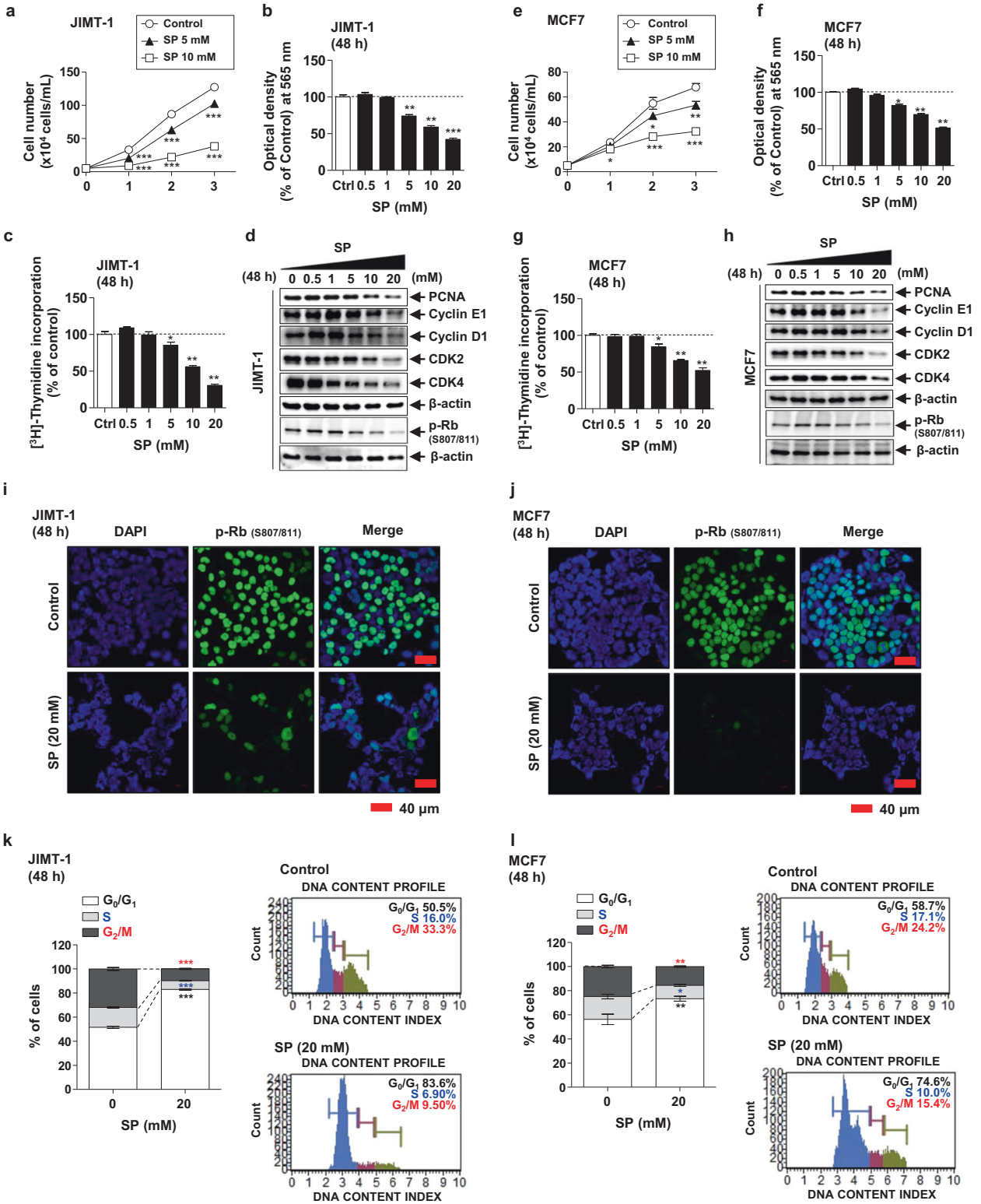

Fig. 1 Effect of sodium propionate (SP) on the proliferation of breast cancer cells. a, **e** Proliferation of JIMT-1 (ER-negative & HER2 expressing) and MCF7 (ER-positive) breast cancer cells in the presence or absence of 5 or 10 mM SP for 1, 2, or 3 days ($n = 5$). Cells were cultured with or without SP (0–20 mM) for 48 h, and viability (3-(4,5-dimethylthiazol-2-yl)-2,5-diphenyltetrazolium bromide [MTT] assay) (**b**, **f**) and DNA synthesis ([^{3}H]-thymidine incorporation assay) (**c**, **g**) were measured ($n = 5$). The effect of SP (0–20 mM) on the levels of the cell cycle proteins proliferating cell nuclear antigen (PCNA), cyclin E1, cyclin D1, cyclin-dependent kinase 2 (CDK2), CDK4, and phospho-retinoblastoma protein (Rb) was examined by Western blotting (**d**, **h**) and immunofluorescence (nuclei, blue; phospho-Rb, green; scale bar = 40 μm; **i**, **j**). Band densities were normalized to those of β-actin. Gel and immunofluorescence images are representative of three independent experiments. **k**, **l** Effect of SP on cell cycle progression (flow cytometry) in JIMT-1 and MCF7 cells ($n = 3$). Data are the mean ± SEM. Significance by Dunnett's test: $^*P < 0.05$, $^{**}P < 0.01$, $^{***}P < 0.001$ vs. the control (Ctrl, no treatment group).

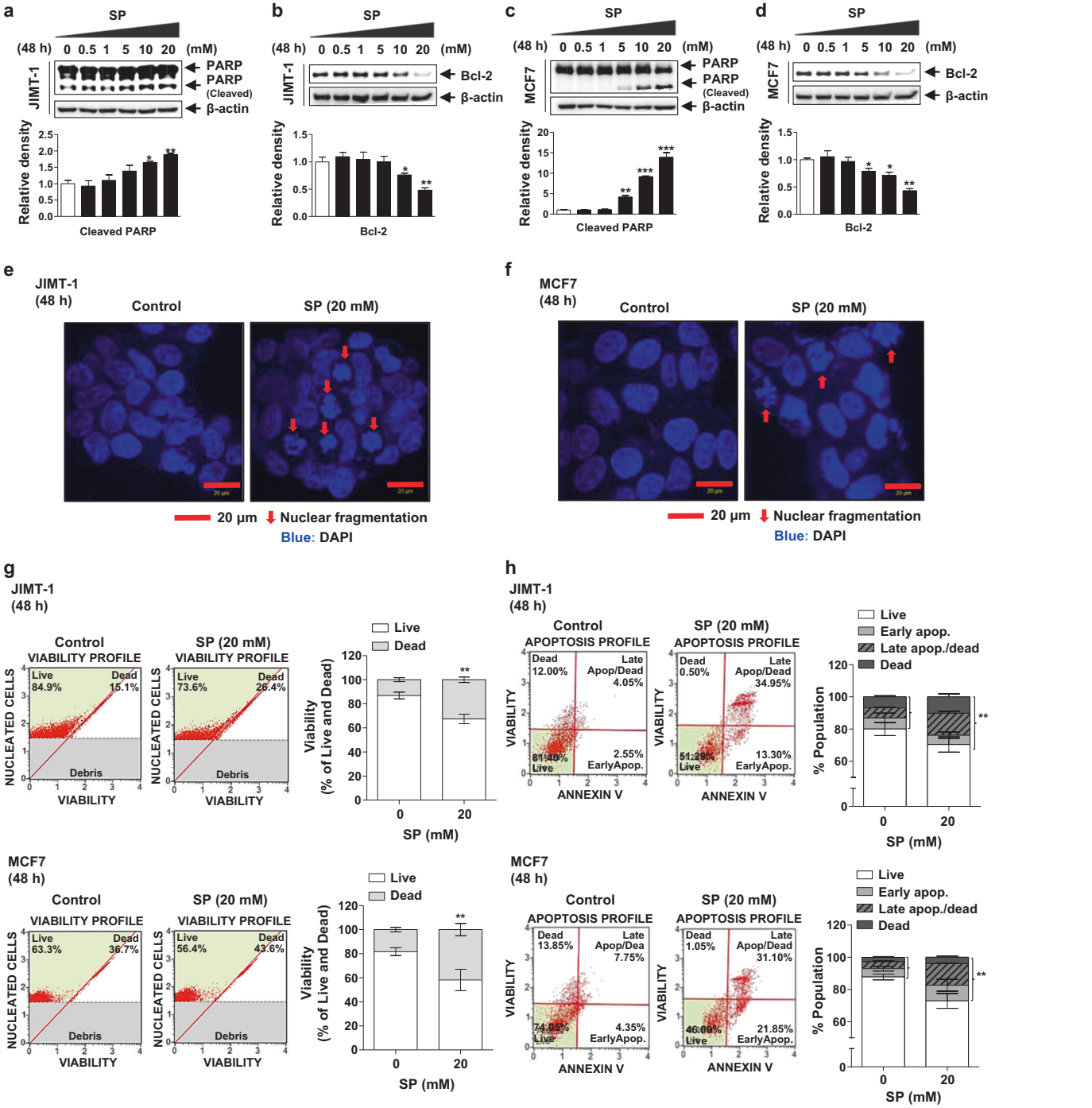

Fig. 2 Effect of SP on the apoptosis of breast cancer cells. a–d Effect of SP on the levels of cleaved poly (ADP-ribose) polymerase (PARP) and B-cell lymphoma 2 (Bcl-2) in JIMT-1 and MCF7 breast cancer cells. Cells were cultured with or without SP (0–20 mM) for 48 h, and apoptosis and survival were examined by measuring the levels of cleaved PARP and Bcl-2, respectively, by Western blotting. Gel images are representative of three independent experiments. Band densities were normalized to those of β-actin. **e**, **f** Effect of SP on nuclear fragmentation in the JIMT-1 and MCF7 breast cancer cells. Nuclei of the cells treated with or without SP (20 mM) were stained with 4′,6-diamidino-2-phenylindole (DAPI) (nuclei, blue; arrow, nuclear fragmentation; scale bar = 20 μm). Immunofluorescence images are representative of three independent experiments. **g** Effect of SP on the viability of the JIMT-1 and MCF7 breast cancer cells. Cells treated with or without SP (20 mM) were mixed with the Muse® Count & Viability reagent, and cell viability was analyzed using Muse® software ($n = 3$). **h** Effect of SP on the proportion of viable and apoptotic JIMT-1 and MCF7 breast cancer cells. Cells treated with or without SP (20 mM) were mixed with Muse® Annexin V and Dead Cell reagent, and the proportions of viable and apoptotic cells were measured using a Muse® Cell Analyzer ($n = 3$). Data are the mean ± SEM. Significance by Dunnett's test: $^*P < 0.05$, $^{**}P < 0.01$ vs. the control (no treatment group).

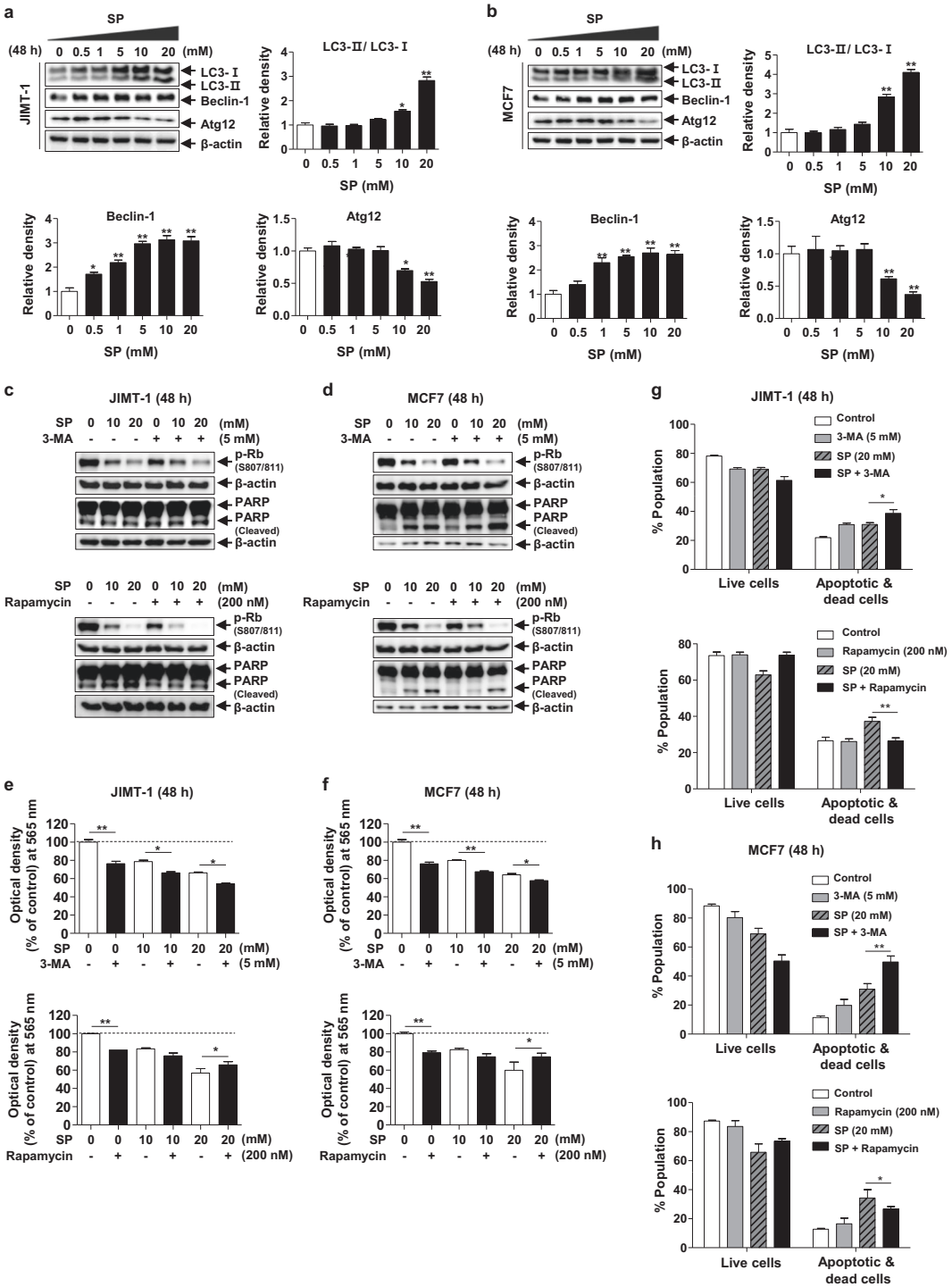

Fig. 3 Effect of SP on autophagy in breast cancer cells. a, **b** Effect of SP on autophagy in JIMT-1 and MCF7 breast cancer cells. Cells were cultured with or without SP (0–20 mM) for 48 h, and the levels of light chain 3 (LC3)-II, beclin-1, and free autophagy-related protein 12 (Atg12) were assessed by Western blotting. **c**, **d** Effect of autophagic regulation on SP-induced apoptosis and proliferation in JIMT-1 and MCF7 breast cancer cells. The levels of phospho-Rb and cleaved PARP were determined by Western blotting in the cells treated with or without SP or 3-MA (autophagy inhibitor) or rapamycin (autophagy activator) for 48 h. Band densities were normalized to those of β-actin. Gel images are representative of three independent experiments. **e**, **f** The viability of the JIMT-1 and MCF7 cells treated with or without SP or autophagic regulators was measured by MTT assays. **g**, **h** Cells were treated with or without SP or autophagic regulators, and the proportions of viable and apoptotic cells were determined using a Muse® Annexin V and Dead Cell Analyzer ($n = 3$). Data are the mean ± SEM. Significance by Dunnett's test: $^{*}P < 0.05$, $^{**}P < 0.01$, $^{***}P < 0.001$ vs. the control (no treatment group) or the indicated group.

proportion of apoptotic cells was increased by 3-MA and decreased by rapamycin in both cell lines (Fig. 3g, h). Therefore, the SP-mediated increase in autophagic activity may be a compensatory mechanism to overcome SP-induced apoptosis.

SP modulates the ROS level in breast cancer cells

Intracellular ROS act as signaling molecules [31]. However, when ROS are maintained at an excessively high level, cell death is induced via oxidative damage [6]. Due to the increase in metabolic rate, gene mutation and relative hypoxia, tumor cells have excessive ROS levels, which are eliminated by increasing antioxidant signaling pathways in the same cells [32]. To determine the role of ROS in SP-induced apoptosis, we measured the ROS levels in the SP-treated breast cancer cells. The ROS levels in the JIMT-1 and MCF7 cells were increased by SP but were abolished by 5 mM NAC (ROS scavenger) (Fig. 4a). Moreover, the antiproliferative effect of SP was attenuated by NAC (Fig. 4b). The SP-mediated decrease in the phospho-Rb levels was not altered by NAC; however, the cleaved PARP levels were decreased (Fig. 4c). When the ROS level increases, Nrf2 induces HO-1 to mediate a reduction of ROS [33]; thus, we measured Nrf2 and HO-1 expression in both cell lines. The expression of Nrf2 and HO-1 was increased by SP (0–20 mM) in the JIMT-1 and MCF7 cells at 48 h in a dose-dependent manner, indicating a compensatory mechanism to overcome the SP-induced apoptosis (Fig. 4d). To investigate the role of HO-1 in the regulation of SP-mediated inhibition of proliferation and apoptosis, we used 25 μM ZnPP (HO-1 inhibitor). The ability of SP to suppress proliferation was enhanced by ZnPP in both cell lines (Fig. 4e). As expected, in the presence of ZnPP, the cleaved PARP level was increased, and Bcl-2 expression was decreased (Fig. 4f). The proportion of apoptotic cells in the SP-treated group was decreased by NAC and increased by ZnPP (Fig. 4g, h). These results indicate that SP induces apoptosis by increasing ROS levels and that cancer cells upregulate HO-1 expression to prevent apoptosis, which may play an important role in the survival of breast cancer cells.

Effects of SP on JAK2-STAT3 and p38 MAPK activation in breast cancer cells

STAT3 is a transcription factor that has multiple pro-oncogenic functions in cancer cells and is mainly activated by JAK-mediated phosphorylation [34]. p38 MAPK plays an important role in the regulation of cancer cell survival, death, differentiation/dedifferentiation, apoptosis, and checkpoint control [35]. SP attenuated the expression and subsequent phosphorylation of JAK2, inhibited the phosphorylation of STAT3 and increased the phosphorylation of p38 in a dose-dependent manner in both cell lines (Fig. 5a, b). These results were confirmed by immunofluorescence (Fig. 5c, d). To determine the relationship between these two signaling proteins, we assessed the phosphorylation levels of STAT3 and p38 at 0–360 min and 0–48 h. At early time points, the phosphorylation level of p38 was increased, whereas that of phospho-STAT3 was unchanged in both cell lines (Fig. 5e, f). Interestingly, the phospho-p38 level increased continuously up to 24 h, and the phosphorylation of STAT3 significantly decreased beginning at 24 h in both cell lines (Fig. 5g, h). These results suggest that SP induces phosphorylation of p38 earlier, and phosphorylation of STAT3 is decreased when p38 activity peaks. The interaction of these two proteins at different time points might constitute a breast cancer cell regulatory mechanism.

SP exerts an anticancer effect by regulating STAT3 and p38 in breast cancer cells

To confirm the roles of STAT3 and p38 in the anticancer effect of SP on JIMT-1 and MCF7 cells, we used inhibitors of STAT3 (100 μM S3I-201) and p38 (10 μM SB203580). Interestingly, S3I-201 enhanced p38 phosphorylation in the cells treated with or without SP, decreased the level of phospho-Rb and increased the levels of cleaved PARP, Nrf2 and HO-1, implying that STAT3 can regulate cell cycle progression, apoptosis and ROS levels (Fig. 6a, b). Thus, SP with S3I-201 resulted in enhanced inhibition of STAT3, leading to potentiation of the anticancer effect of SP. Similar to that of S3I-201, the anticancer effect of SP was due to direct activation of p38. When p38 upregulation in the SP-treated cells was inhibited by SB203580, the levels of phospho-STAT3, phospho-Rb, Nrf2 and HO-1 were unchanged. However, the SP-mediated increases in the levels of cleaved PARP were decreased by SB203580 in the JIMT-1 and MCF7 cells. In the presence of NAC, the ability of SP to phosphorylate p38 and increase the expression of Nrf2 and HO-1 was weakened, while phospho-STAT3 was not affected in both cell lines, implying that ROS can regulate p38 activation and induce the antioxidant pathway (Fig. 6c). S3I-201, but not SB203580, increased the ROS level and decreased cell viability, which was ameliorated by NAC (Fig. 6d, e), indicating the involvement of the STAT3-ROS-p38 signaling axis. SB203580 did not alter the viability of either cell line because it did not affect the ROS levels. Compared with that of the control, the proportion of apoptotic cells was increased by S3I-201 alone, and STAT3 regulation (S3I-201) potentiated the SP-induced apoptosis in both cell lines (Fig. 6f). However, SB203580 did not alter the proportion of apoptotic cells, and p38 regulation (SB203580) decreased the SP-induced apoptosis (Fig. 6g). These results suggest that the inhibition of STAT3 activity by SP exerts an anticancer effect by increasing the ROS level and activating p38. Thus, an elevated ROS level and sustained p38 activation are implicated in the SP-induced apoptosis of breast cancer cells.

SP inhibits tumor growth in a breast cancer cell xenograft model

To confirm the ability of SP to suppress tumor growth in vivo, we injected JIMT-1 or MCF7 cells into athymic nude mice. Tumor growth in the SP-administered JIMT-1 group was slower than that in the JIMT-1 control group (Fig. 7a). Similarly, the growth of tumors derived from the MCF7 cells was significantly reduced by SP compared with that of the MCF7 control group (Fig. 7e). SP also reduced the tumor weight by 50% (Fig. 7b, f) and the tumor size (Fig. 7c, g) compared with the control, regardless of whether the tumors were derived from JIMT-1 or MCF7 cells. The regulatory effects on STAT3 and p38 showed the same patterns in vitro and in vivo (Fig. 7d, h). These results indicate that SP suppressed tumor growth by regulating STAT3 and p38 MAPK in JIMT-1 and MCF7 breast cancer cells.

DISCUSSION

Our findings suggest that the regulation of JAK2-STAT3-ROS-p38 MAPK signaling pathways could be an effective therapeutic strategy for breast cancer and confirm the potential of SP for the treatment of breast cancer. Our study yielded three major findings (Fig. 7i). First, SP exerted an anticancer effect by inducing cell cycle arrest and apoptosis in breast cancer cells, to which breast cancer cells responded by increasing autophagy and Nrf2 and HO-1 expression. Second, the antiproliferative effect of SP in breast cancer cells was mediated by inhibition of JAK2-STAT3, which led to increased intracellular ROS generation, in turn resulting in apoptosis. Third, the relationship between ROS generation and long-term activation of p38 was regulated by SP-induced STAT3 inhibition, resulting in apoptosis of breast cancer cells. This is the first report of the mechanism of the anticancer effect of SP, the sodium salt of propionate, which is produced from indigestible carbohydrates by bacteria resident in the human gut.

The suppression of proliferation and induction of apoptosis in cancer cells have been investigated as anticancer therapies [36, 37]. Although many studies have used small molecule inhibitors of cancer cell proliferation as anticancer drugs [38], we focused on SP, which is used as a food additive. SP significantly

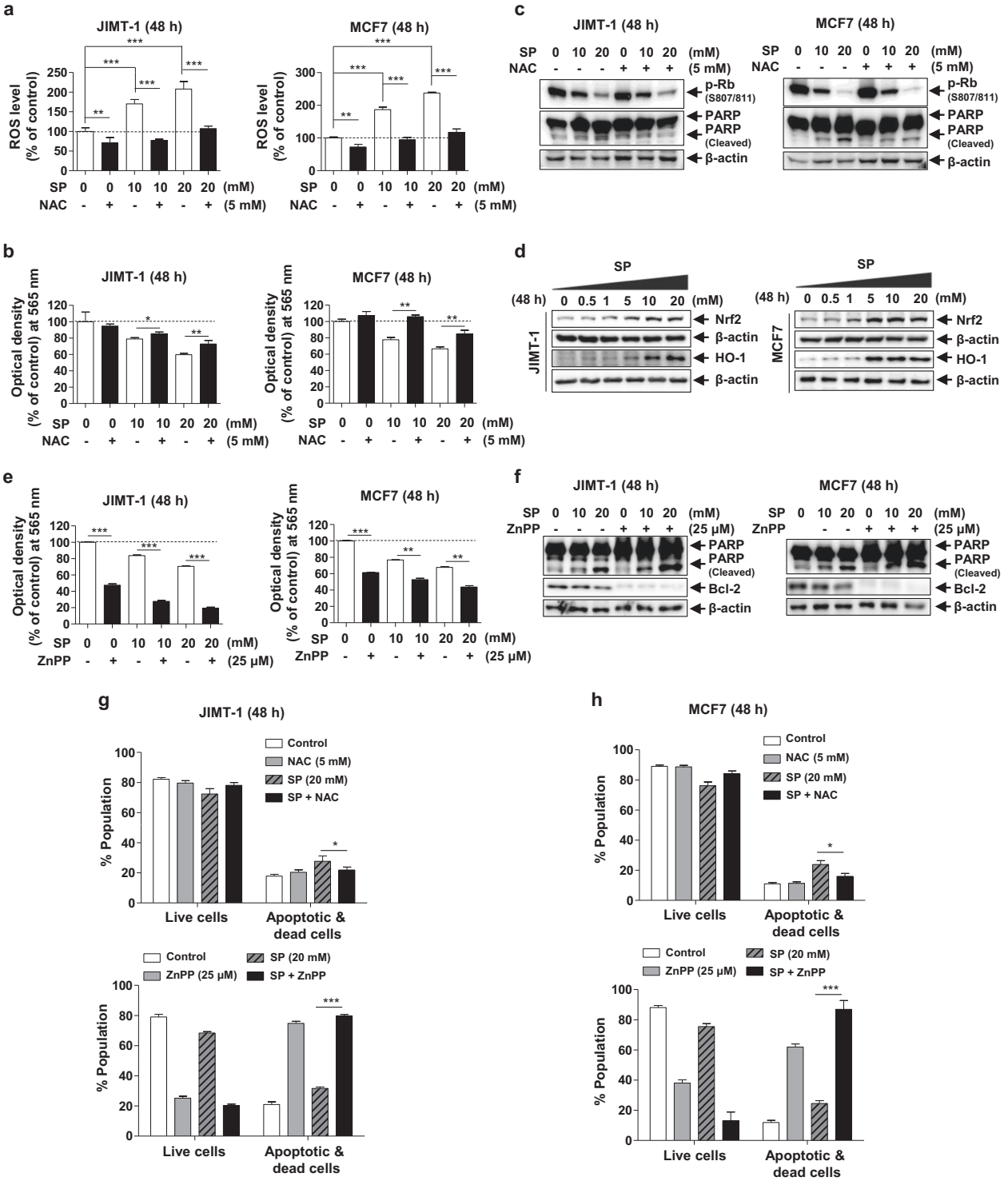

Fig. 4 Effects of reactive oxygen species (ROS) on SP-induced proliferation and apoptosis in breast cancer cells. a, **b** Effect of SP on ROS production and viability in JIMT-1 and MCF7 breast cancer cells. The ROS level was measured in the cells treated with or without SP (10 or 20 mM) or *N*-acetyl-*L*-cysteine (NAC; 5 mM, ROS scavenger) for 48 h by 2′,7′-dichlorofluorescin diacetate (H_2DCFDA) assays ($n = 3$). Viability was determined in the cells treated with or without SP or NAC by MTT assays ($n = 3$). **c** Effect of NAC on SP-induced apoptosis and proliferation. The levels of cleaved PARP and phospho-Rb were measured in the cells treated with or without SP or NAC. **d** Effect of SP on the expression of nuclear factor erythroid 2-related factor 2 (Nrf2) and heme oxygenase 1 (HO-1). Nrf2 and HO-1 expression was assessed in the cells treated with or without SP (0–20 mM) by Western blotting. Band densities were normalized to those of β-actin. Gel images are representative of three independent experiments. **e** Effect of zinc protoporphyrin IX (ZnPP; HO-1 inhibitor) on the SP-induced proliferation. The viability of the cells treated with or without SP or ZnPP (25 μM) for 48 h was measured by MTT assays ($n = 3$). **f** Effect of ZnPP on the SP-induced apoptosis and proliferation. The levels of cleaved PARP and Bcl-2 were assessed by Western blotting in the cells treated with or without SP or ZnPP ($n = 3$). **g**, **h** Effect of NAC or ZnPP on the SP-induced apoptosis. The proportion of viable and apoptotic cells treated with or without SP, NAC or ZnPP was determined using a Muse® Annexin V and Dead Cell Analyzer ($n = 3$). Data are the mean ± SEM. Significance by Dunnett's test: $^*P < 0.05$, $^{**}P < 0.01$, $^{***}P < 0.001$ vs. the indicated group.

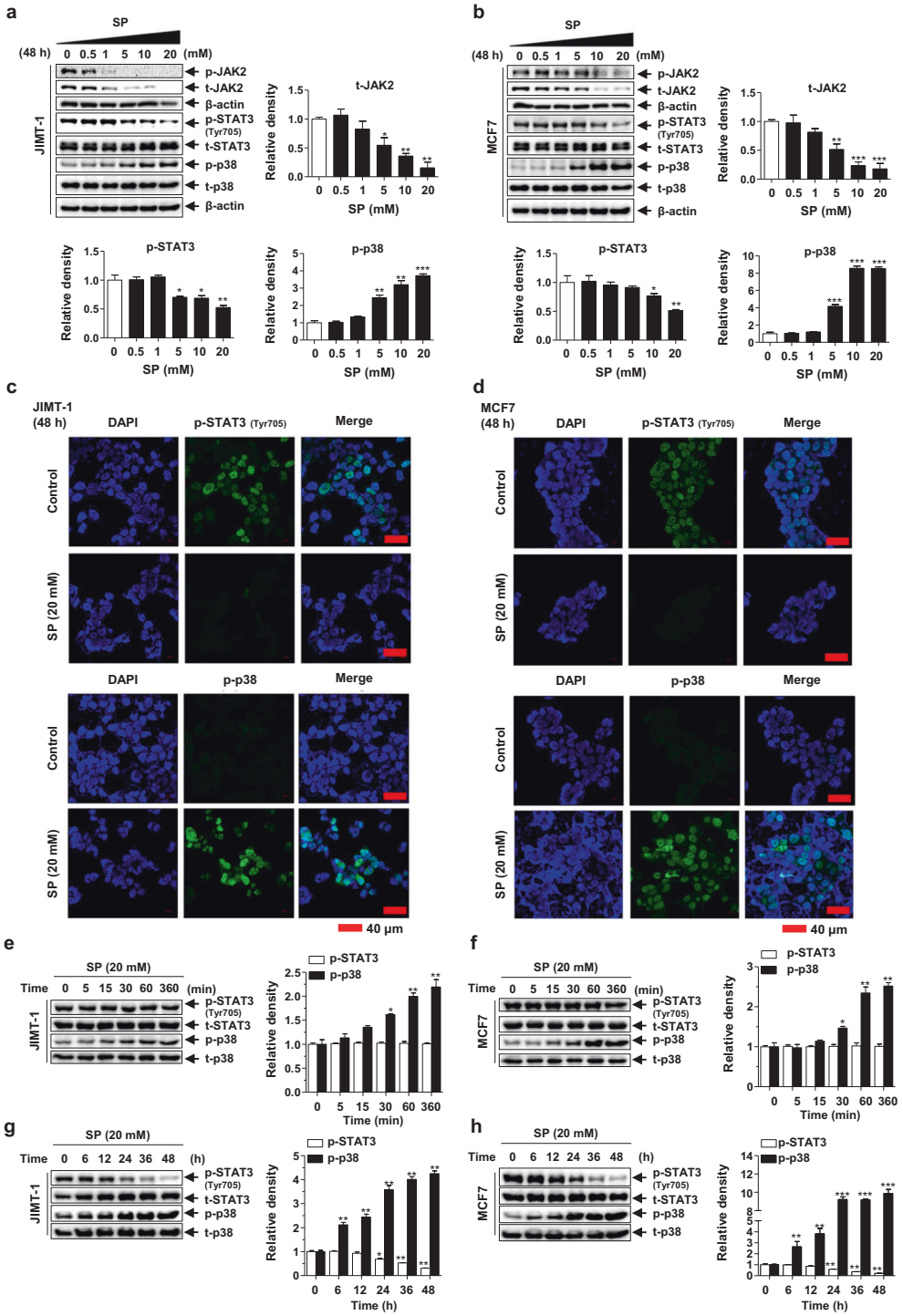

Fig. 5 Effects of SP on Janus kinase 2 (JAK2)-signal transducer and activator of transcription 3 (STAT3) and p38 mitogen-activated protein kinase (MAPK) activation in breast cancer cells. a, **b** Effect of SP on the expression and phosphorylation of JAK2, STAT3 and p38 in JIMT-1 and MCF7 breast cancer cells. Cells cultured with or without SP (0–20 mM) for 48 h were lysed, and the lysates were subjected to Western blotting using the indicated antibodies. Gel images are representative of five independent experiments. **c**, **d** The cells treated with or without SP (20 mM) were incubated with primary antibodies for phospho-p38 and phospho-STAT3 (green), followed by a fluorescein isothiocyanate (FITC)-conjugated secondary antibody and DAPI (blue, nuclei). Immunofluorescence images are representative of three independent experiments (scale bar = 40 μm). The levels of phospho-p38 and phospho-STAT3 in the JIMT-1 and MCF7 cells treated with 20 mM SP for 0–360 min (**e**, **f**) or 0–48 h (**g**, **h**) were assessed by Western blotting ($n = 5$). The intensity of the phosphorylated protein bands was normalized to that of the total protein or β-actin. Data are the mean ± SEM. Significance by Dunnett's test: $^{*}P < 0.05$, $^{**}P < 0.01$, $^{***}P < 0.001$ vs. the control (no treatment or 0 time-point group).

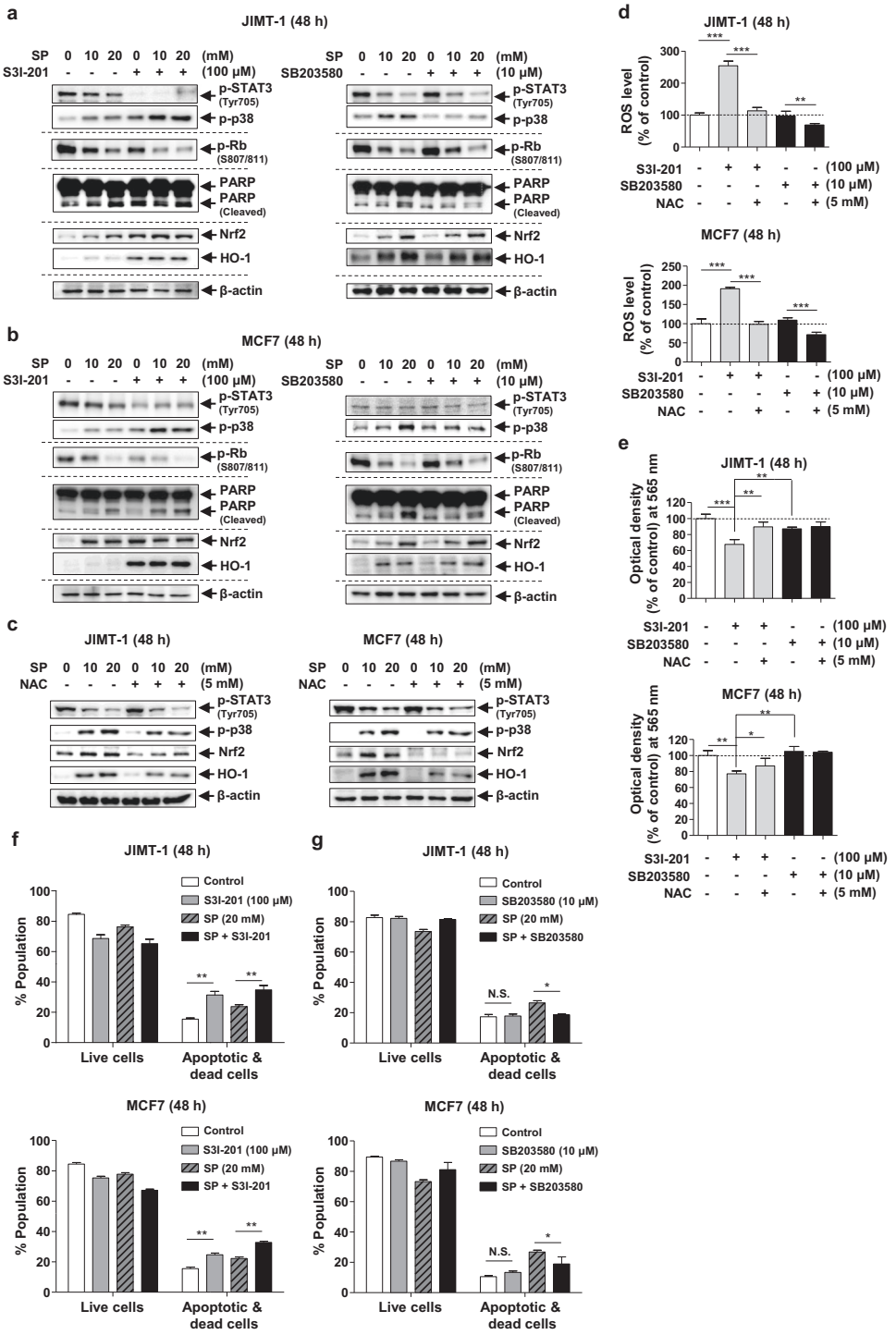

Fig. 6 Effects of STAT3 and p38 regulation on SP-induced ROS generation, proliferation and apoptosis in breast cancer cells. a, **b** JIMT-1 and MCF7 cells were cultured with or without SP (10 or 20 mM), S3I-201 (100 μM, STAT3 inhibitor) or SB203580 (10 μM, p38 inhibitor) for 48 h. Cell lysates were subjected to Western blotting using the indicated antibodies. **c** Effects of NAC on SP-induced phosphorylation of p38 and STAT3 in JIMT-1 and MCF7 cells. The levels of p38 and STAT3 phosphorylation and the expression of Nrf2 and HO-1 were determined in the cells treated with or without SP or NAC by Western blotting. Band densities were normalized to those of β-actin. Gel images are representative of three independent experiments. **d**, **e** Effects of STAT3 or p38 inhibitors on ROS production and cell viability. ROS levels and viability were determined in the cells treated with or without S3I-201, SB203580, or NAC (5 mM, ROS scavenger) by H_2DCFDA and MTT assays, respectively ($n = 3$). **f**, **g** The proportions of viable and apoptotic JIMT-1 or MCF7 cells treated with or without SP, S3I-201, or SB203580 were determined using a Muse® Annexin V and Dead Cell Analyzer ($n = 3$). Data are the mean ± SEM. Significance by Dunnett's test: $^*P < 0.05$; $^{**}P < 0.01$; $^{***}P < 0.001$ vs. the indicated group. N.S., not significant.

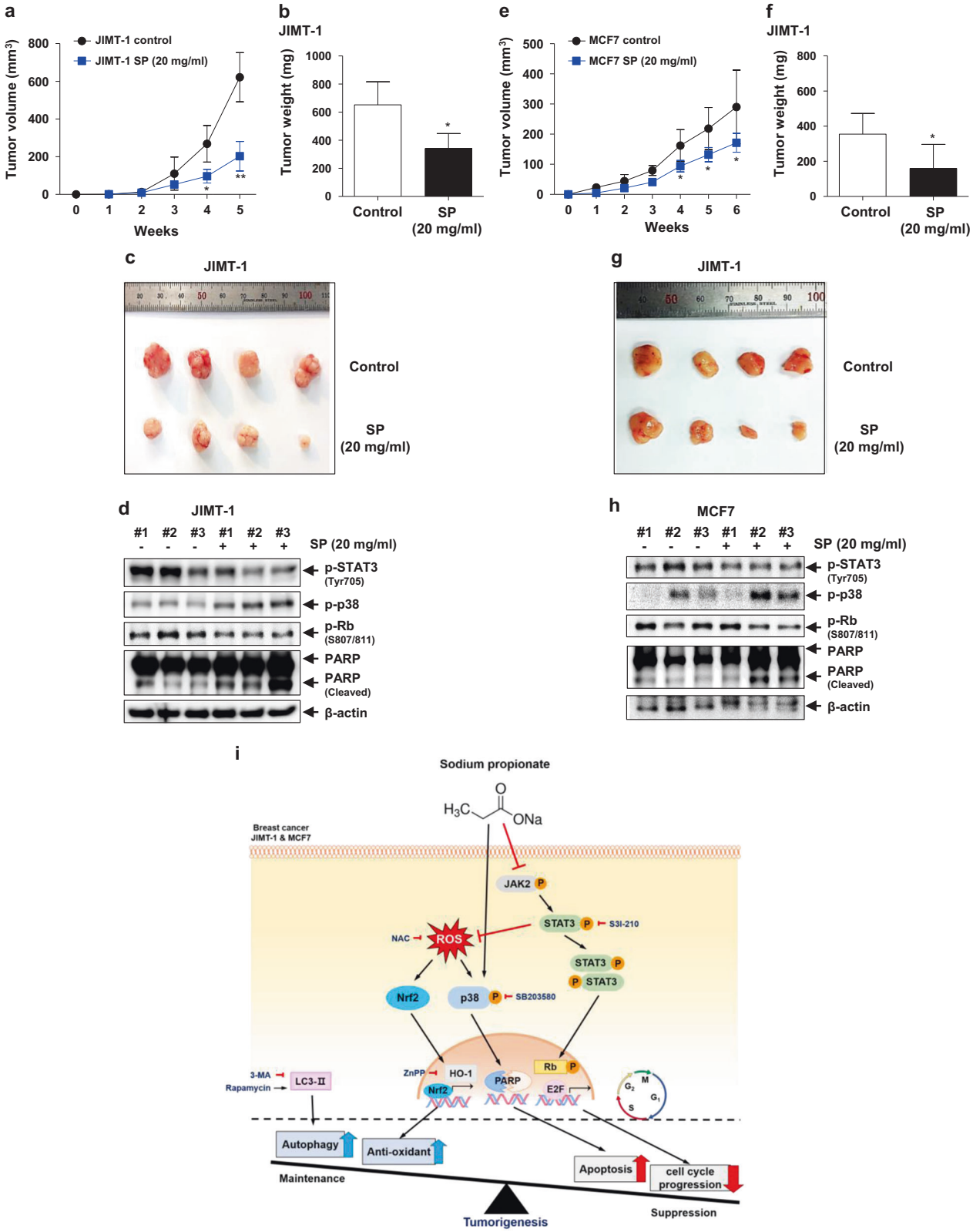

Fig. 7 Inhibitory effect of SP on tumor growth. Equal numbers of JIMT-1 and MCF7 cells were inoculated into the right flank of 5- or 6-week-old female athymic NCr-*nu/nu* mice ($n = 5$). Administration of 20 mg/mL SP in drinking water was started simultaneously with injection of cells. **a**, **e** Tumor sizes were measured weekly, and the rates of tumor growth were compared. **b**, **f** Tumors were dissected, and their weights were determined. **c**, **g** Representative photographs of the dissected tumors. **d**, **h** Tumors were lysed, and the lysates were subjected to Western blotting using the indicated antibodies ($n = 3$). Data are the mean ± SEM. Significance by Dunnett's test: $^{*}P < 0.05$, $^{**}P<0.01$ vs. the control (no SP treatment). **i** Proposed mechanism of action of SP in the suppression of tumor growth by inhibiting the proliferation and promoting the apoptosis of breast cancer cells.

inhibited cell proliferation regardless of subtype (Fig. 1a, e, Supplementary Fig. S1). In addition, SP induced cell cycle arrest at G_0/G_1, which inhibited cell cycle-regulated protein activation (Fig. 1) and induced apoptosis by enhancing PARP cleavage and decreasing Bcl-2 expression in both the JIMT-1 and MCF7 cells (Fig. 2). Notably, the suppression of proliferation and induction of apoptosis in breast cancer cells were independent of the GPR41- and GPR43-mediated signaling pathways (Supplementary Fig. S2). Therefore, the ability of SP to inhibit cancer growth warrants further investigation.

The regulation of autophagy has received increased attention as a tumor suppressor or tumor promoter [39]. The induction of apoptosis by downregulating autophagy and the cytoprotective effect in response to a toxic stimulus with the aim of alleviating cellular stress are possible strategies [40]. SP increased the autophagic activity of breast cancer cells (Fig. 3a, b), and an activator of autophagy (rapamycin) inhibited SP-induced apoptosis (Fig. 3c–h). Therefore, these results suggest that the SP-mediated increase in autophagic activity is a compensatory response to overcome SP-induced apoptosis for the survival of breast cancer cells.

Although ROS at normal levels function as messengers in intracellular signaling pathways [31], an excessive ROS level induces apoptosis by causing intracellular oxidative damage [41]. Conversely, blockade of ROS production prevents intracellular signaling [31]. In this study, SP increased the ROS level in breast cancer cells, and a decreased ROS level inhibited SP-induced apoptosis (Fig. 4a–c). Interestingly, the expression of the antioxidant proteins Nrf2 and HO-1 was increased by SP, and the inhibition of HO-1 expression significantly promoted the SP-induced apoptosis of breast cancer cells (Fig. 4d–h). Thus, SP increased the ROS level, which induced apoptosis in breast cancer cells, and Nrf2 and HO-1 expression was increased to maintain cell survival. Although both autophagic activity and antioxidant levels were increased by SP, this change cannot overcome the apoptosis of breast cancer cells. Therefore, the ability of SP to increase intracellular ROS generation mediates its main anticancer effect against breast cancer cells.

Next, we focused on the molecular mechanisms of the SP-induced antiproliferative effects and apoptosis of breast cancer cells. Interestingly, SP decreased the expression and phosphorylation of JAK2. Although JAK2 is known to be negatively regulated by the ubiquitin-proteasome pathway [42], further study of the SP-mediated JAK2 ubiquitination is needed. In addition, SP decreased STAT3 activation and induced and maintained p38 activation after 12 h (Fig. 5). The knockdown or blockade of STAT3 increased the ROS levels and induced apoptosis in breast cancer cells [43]. ROS-induced p38 activation induced apoptosis in breast cancer cells [44, 45]. In this study, ROS generation, p38 MAPK activation, and Nrf2 and HO-1 expression were increased in the breast cancer cells treated with both SP and a STAT3 inhibitor, resulting in inhibition of phospho-Rb and promotion of apoptosis, whereas STAT3 activity, Rb phosphorylation, and ROS generation were not affected in the cells treated with a p38 inhibitor (Fig. 6). Thus, the SP-induced increase in ROS generation is mainly caused by inhibition of STAT3. Compared with S3I–201 alone, SP with S3I-201 increased p38 phosphorylation without affecting Nrf2 and HO-1 expression, indicating direct activation of p38 by SP. Therefore, SP-induced STAT3 inhibition plays an important role in cell cycle arrest, and direct stimulation of ROS generation and activation of p38 lead to apoptosis. These in vitro results were confirmed in cancer tissues (Fig. 7d, h).

In conclusion, SP inhibits JAK2-STAT3 activation, causing cell cycle arrest, and stimulates ROS generation, leading to p38 activation and apoptosis in breast cancer cells. To compensate, breast cancer cells induce autophagy and antioxidant pathways (Nrf2 and HO-1) to prevent apoptosis; however, this process does not counteract the anticancer effect of SP. Therefore, SP is a potential candidate for the management of breast cancer through the regulation of the JAK2-STAT3-ROS-p38 MAPK signaling pathway. This study provides insight into a novel therapeutic strategy for breast cancer.

ACKNOWLEDGEMENTS

This work was supported by the National Research Foundation of Korea (KRF), funded by the Ministry of Science and ICT (grant no. NRF-2018R1A2A2A05023578).

AUTHOR CONTRIBUTIONS

JHH, HSP, KSH, and CSM designed the study, analyzed the data, and wrote the manuscript. JHH, KSH, and CSM revised the manuscript. JHH, HSP, JWP, DHL, KWJ, and ML performed the experiments and analyzed the data.

ADDITIONAL INFORMATION

The online version of this article (https://doi.org/10.1038/s41401-020-00522-2) contains supplementary material, which is available to authorized users.

Competing interests: The authors declare no competing interests.

REFERENCES

1. DeSantis CE, Ma J, Gaudet MM, Newman LA, Miller KD, Sauer AG, et al. Breast cancer statistics, 2019. CA Cancer J Clin. 2019;69:438–51.
2. Harbeck N, Penault-Llorca F, Cortes J, Gnant M, Houssami N, Poortmans P, et al. Breast cancer. Nat Rev Dis Prim. 2019;5:66.
3. Malumbres M, Barbacid M. Cell cycle, CDKs and cancer: a changing paradigm. Nat Rev Cancer. 2009;9:153–66.
4. Evan GI, Vousden KH. Proliferation, cell cycle and apoptosis in cancer. Nature. 2001;411:342–8.
5. Fragomeni SM, Sciallis A, Jeruss JS. Molecular subtypes and local-regional control of breast cancer. Surg Oncol Clin N Am. 2018;27:95–120.
6. Schieber M, Chandel NS. ROS function in redox signaling and oxidative stress. Curr Biol. 2014;24:R453–62.
7. Sarkar S, Ravikumar B, Rubinsztein DC. Autophagic clearance of aggregate-prone proteins associated with neurodegeneration. Methods Enzymol. 2009;453:83–110.
8. Namba T, Takabatake Y, Kimura T, Takahashi A, Yamamoto T, Matsuda J, et al. Autophagic clearance of mitochondria in the kidney copes with metabolic acidosis. J Am Soc Nephrol. 2014;25:2254–66.
9. Mizushima N. Autophagy: process and function. Genes Dev. 2007;21:2861–73.
10. Levy JMM, Towers CG, Thorburn A. Targeting autophagy in cancer. Nat Rev Cancer. 2017;17:528–42.
11. Poillet-Perez L, Despouy G, Delage-Mourroux R, Boyer-Guittaut M. Interplay between ROS and autophagy in cancer cells, from tumor initiation to cancer therapy. Redox Biol. 2015;4:184–92.
12. Ma JH, Qin L, Li X. Role of STAT3 signaling pathway in breast. Cell Commun Signal. 2020;18:33.
13. Wake MS, Watson CJ. STAT3 the oncogene—still eluding therapy? FEBS J. 2015;282:2600–11.
14. Kralova J, Dvorak M, Koc M, Kral V. p38 MAPK plays an essential role in apoptosis induced by photoactivation of a novel ethylene glycol porphyrin derivative. Oncogene. 2008;27:3010–20.
15. Deng YT, Huang HC, Lin JK. Rotenone induces apoptosis in MCF-7 human breast cancer cell-mediated ROS through JNK and p38 signaling. Mol Carcinog. 2010;49:141–51.
16. Ivanov VN, Ronai Z. p38 protects human melanoma cells from UV-induced apoptosis through down-regulation of NF-κB activity and Fas expression. Oncogene. 2000;19:3003–12.
17. Jiang X, Tang J, Wu M, Chen S, Xu Z, Wang H, et al. BP1102 exerts an antitumor effect on the AGS human gastric cancer cell line through modulating the STAT3 and MAPK signaling pathways. Mol Med Rep. 2019;19:2698–706.
18. Wang JR, Luo YH, Piao XJ, Zhang Y, Feng YC, Li JQ, et al. Mechanisms underlying isoliquiritigenin-induced apoptosis and cell cycle arrest via ROS-mediated MAPK/STAT3/NF-κB pathways in human hepatocellular carcinoma cells. Drug Dev Res. 2019;80:461–70.
19. Darvin P, Joung YH, Kang DY, Sp N, Byun HJ, Hwang TS, et al. Tannic acid inhibits EGFR/STAT1/3 and enhances p38/STAT1 signalling axis in breast cancer cells. J Cell Mol Med. 2017;21:720–34.

20. Hurst NR, Kendig DM, Murthy KS, Grider JR. The short chain fatty acids, butyrate and propionate, have differential effects on the motility of the guinea pig colon. Neurogastroenterol Motil. 2014;26:1586–96.
21. Sun M, Wu W, Liu Z, Cong Y. Microbiota metabolite short chain fatty acids, GPCR, and inflammatory bowel diseases. J Gastroenterol. 2017;52:1–8.
22. Koh A, De Vadder F, Kovatcheva-Datchary P, Backhed F. From dietary fiber to host physiology: short-chain fatty acids as key bacterial metabolites. Cell. 2016;165:1332–45.
23. Han JH, Kim IS, Jung SH, Lee SG, Son HY, Myung CS. The effects of propionate and valerate on insulin responsiveness for glucose uptake in 3T3-L1 adipocytes and C2C12 myotubes via G protein-coupled receptor 41. PLoS One. 2014;9:e95268.
24. Bindels LB, Porporato P, Dewulf EM, Verrax J, Neyrinck AM, Martin JC, et al. Gut microbiota-derived propionate reduces cancer cell proliferation in the liver. Br J Cancer. 2012;107:1337–44.
25. Tang Y, Chen Y, Jiang H, Robbins GT, Nie D. G-protein-coupled receptor for short-chain fatty acids suppresses colon cancer. Int J Cancer. 2011;128:847–56.
26. Thirunavukkarasan M, Wang C, Rao A, Hind T, Teo YR, Siddiquee AA, et al. Short-chain fatty acid receptors inhibit invasive phenotypes in breast cancer cells. PLoS One. 2017;12:e0186334.
27. Park HS, Quan KT, Han JH, Jung SH, Lee DH, Jo E, et al. Rubiarbonone C inhibits platelet-derived growth factor-induced proliferation and migration of vascular smooth muscle cells through the focal adhesion kinase, MAPK and STAT3 Tyr^{705} signalling pathways. Br J Pharmacol. 2017;174:4140–54.
28. Toma S, Emionite L, Scaramuccia A, Ravera G, Scarabelli L. Retinoids and human breast cancer: in vivo effects of an antagonist for RAR-α. Cancer Lett. 2005;219:27–31.
29. Qiang L, Zhao B, Ming M, Wang N, He T, Hwang S, et al. Regulation of cell proliferation and migration by p62 through stabilization of Twist1. Proc Natl Acad Sci U S A. 2014;111:9241–6.
30. Salabei JK, Hill BG. Autophagic regulation of smooth muscle cell biology. Redox Biol. 2015;4:97–103.
31. Schieber Sauer H, Wartenberg M, Hescheler J. Reactive oxygen species as intracellular messengers during cell growth and differentiation. Cell Physiol Biochem. 2001;11:173–86.
32. Perillo B, Di Donato M, Pezone A, Di Zazzo E, Giovannelli P, Galasso G, et al. ROS in cancer therapy: the bright side of the moon. Exp Mol Med. 2020;52:192–203.
33. Zimta AA, Cenariu D, Irimie A, Magdo L, Nabavi SM, Atanasov AG. The role of Nrf2 activity in cancer development and progression. Cancers. 2019;11:1755.
34. Koul HK, Pal M, Koul S. Role of p38 MAP kinase signal transduction in solid tumors. Genes Cancer. 2013;4:342–59.
35. Avalle L, Camporeale A, Camperi A, Poli V. STAT3 in cancer: a double edged sword. Cytokine. 2017;98:42–50.
36. Pfeffer CM, Singh ATK. Apoptosis: a target for anticancer therapy. Int J Mol Sci. 2018;19:448.
37. Ming YL, Song G, Chen LH, Zheng ZZ, Chen ZY, Ouyang GL, et al. Anti-proliferation and apoptosis induced by a novel intestinal metabolite of ginseng saponin in human hepatocellular carcinoma cells. Cell Biol Int. 2007;31:1265–73.
38. Hoelder S, Clarke PA, Workman P. Discovery of small molecule cancer drugs: successes, challenges and opportunities. Mol Oncol. 2012;6:155–76.
39. Thorburn A, Thamm DH, Gustafson DL. Autophagy and cancer therapy. Mol Pharmacol. 2014;85:830–8.
40. Fulda S. Autophagy in cancer therapy. Front Oncol. 2017;7:128.
41. Simon HU, Haj-Yehia A, Levi-Schaffer F. Role of reactive oxygen species (ROS) in apoptosis induction. Apoptosis. 2000;5:415–8.
42. Ungureanu D, Saharinen P, Junttila I, Hilton DJ, Silvennoinen O. Regulation of Jak2 through the ubiquitin-proteasome pathway involves phosphorylation of Jak2 on Y1007 and interaction with SOCS-1. Mol Cell Biol. 2002;22:3316–26.
43. Lu L, Dong J, Wang L, Xia Q, Zhang D, Kim H, et al. Activation of STAT3 and Bcl-2 and reduction of reactive oxygen species (ROS) promote radioresistance in breast cancer and overcome of radioresistance with niclosamide. Oncogene. 2018;37:5292–304.
44. Yang LH, Ho YJ, Lin JF, Yeh CW, Kao SH, Hsu LS. Butein inhibits the proliferation of breast cancer cells through generation of reactive oxygen species and modulation of ERK and p38 activities. Mol Med Rep. 2012;6:1126–32.
45. Zhai JW, Gao C, Ma WD, Wang W, Yao LP, Xia XX, et al. Geraniin induces apoptosis of human breast cancer cells MCF-7 via ROS-mediated stimulation of p38 MAPK. Toxicol Mech Methods. 2016;26:311–8.